

Design and Stability Analysis of Buck-Boost Converter Applied with Adaptive Voltage Positioning Technique

Fei Deng¹, Guangjun Xie^{1,2} and Xin Cheng^{1,2*}

¹*School of Electronic Science and Applied Physics, Hefei University of Technology, Hefei, China*

²*State Key Lab of ASIC and System, Fudan University, Shanghai, China*
**ceciliacheng1017@163.com*

Abstract

In this paper a buck-boost converter with adaptive voltage positioning (AVP) control technique is researched. According to the small-signal model of the converter, a constant output impedance required in AVP control is realized. Besides, the RHP zero in buck-boost converter is analyzed and the design of compensator to keep the system stable is presented. The converter is simulated in Simulink and the simulation results verify the above analysis.

Keywords: *AVP control, buck-boost converter, constant output impedance, RHP zero, stability*

1. Introduction

With the increasing speed and capacity of data processing in CPU, DSP and other modules, their demands for power supply with large value and fast response of output current and small overshoot or undershoot of output voltage become more stringent [1, 2]. For this case, some control techniques such as V^2 control, hysteretic control, or multi-channel buck topology are utilized to improve static and dynamic performance [3-5]. The major contributions of [3] is to characterize digital V^2 control with different ramp compensations, and propose a hybrid-ramp compensation concept for reducing the current sensing gain requirements for the stability issue. A buck-boost converter with a positive output voltage is presented in [5], which combines the KY converter (a novel voltage-bucking/boosting converter) and the traditional synchronously rectified (SR) buck converter. The problem in voltage bucking of the KY converter can be solved, thereby increasing the application capability of the KY converter. However, if a very low voltage and a very fast current are required, the peak-peak value of output voltage must be reduced, which can be achieved by using a large output capacity with low equivalent series resistance (ESR), while it results in a large area and a low power density.

In order to solve the problem above, adaptive voltage positioning (AVP) control technique is widely used in buck converters [4, 6, 7] because it has plenty of advantages such as smaller output capacitor, lower power dissipation and constant output impedance. To improve other VRM features, a novel hysteretic controller has been proposed in [4]. The controller includes both an output voltage-regulation compensator network, and an adaptive voltage-positioning compensator network. The method reduces the steady-state switching frequency deviations at different loads and achieves a robust transient response performance. In [6], a novel scheme AVP+ is analyzed, this scheme provides better stability margin and output impedance performance.

Figure 1 gives the transient waveform of buck converter with AVP control, which shows

that it eliminates ringing effect of output voltage, thus the overshoot and undershoot voltages can be reduced apparently. In addition, the transient response time of AVP control system depends on the rising time of inductor current and is faster than traditional control schemes.

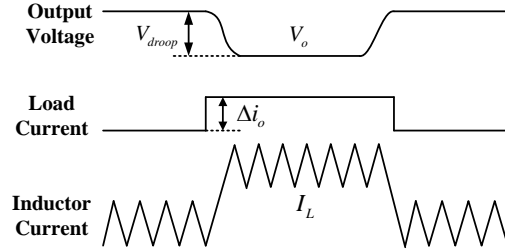


Figure 1. Transient Waveform of Buck Converter with AVP Control

However, for boost and buck-boost converter, a right-half-plane (RHP) zero exists in their control-to-output transfer functions, which limits the bandwidth and response time. Besides, the boost and buck-boost converters will induce a larger voltage drop in load transient compared with buck converter, because the energy cannot be delivered to output voltage when the power switch is turned on. Therefore, boost and buck-boost converters work with worse transient performance because of their narrower bandwidth and larger overshoot or undershoot voltage [8, 9]. Although the transient performance of boost and buck-boost converters can be efficiently improved with AVP control, the system stability would also be influenced by the RHP zero. Therefore, it is necessary to study the design of AVP controlled boost and buck-boost converters.

2. AVP Control Technique

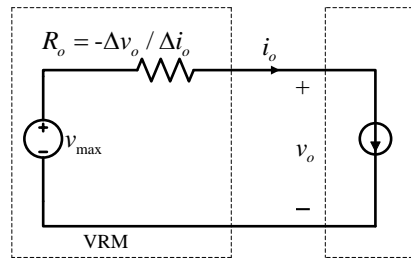


Figure 2. The Equivalent Circuit of VRM

As shown in Figure 2, AVP control technique is used to improve dynamic performance and reduce area cost by realizing a constant output impedance R_o of voltage regulator module (VRM), which means that the output voltage v_o decreases when the output current i_o increases, and vice versa [10]. From

$$R_o = - \frac{\Delta v_o}{\Delta i_o} \quad (1)$$

and

$$v_o = v_{\max} - i_o R_o \quad (2)$$

It can be seen that the AVP technique can be realized by a voltage control loop and a current control loop when they satisfy

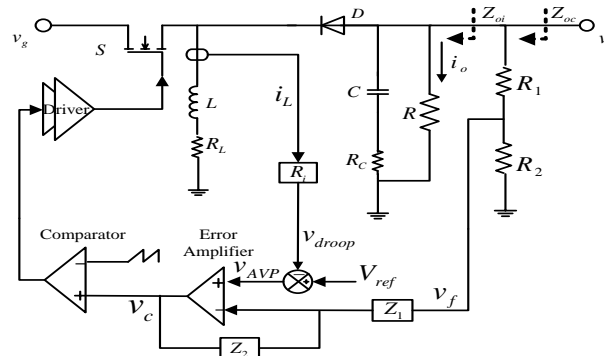
$$v_o = v_{ref} = v_{\max} - i_{ref} R_o = v_{\max} - i_o R_o \quad (3)$$

3. Design of buck-boost Converter with AVP Control

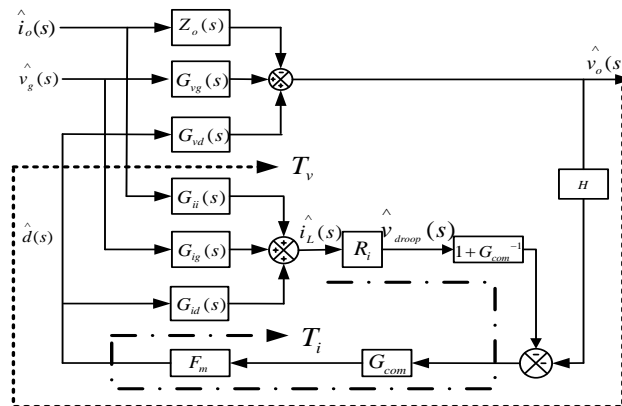
3.1. Small Signal Model of Buck-boost Converter

The schematic of buck-boost converter with AVP control technique is illustrated in Figure 3(a) [11, 12]. By transforming the sensed inductor current i_L into the voltage v_{droop} , and subtracting it from the reference voltage v_{ref} , an AVP control voltage v_{AVP} is achieved. Both the AVP control voltage v_{AVP} and the output voltage v_o decrease when the inductor current increases, thus a constant output impedance is achieved.

This paper takes buck-boost converter for example to study the design and stability analysis with AVP control. It is organized as follows. Section 2 introduces the AVP control and Section 3 discusses the design of buck-boost converter with AVP control. Simulation results are presented in Section 4. Finally, the conclusion of this paper is generalized in Section 5.



(a) Schematic



(b) Small-signal Model

Figure 3. Buck-boost Converter with AVP Control

Figure 3(b) shows the small-signal model of buck-boost converter illustrated in Figure 3(a), where H is the feedback gain decided by resistors R_1 and R_2 , G_{com} represents the compensator, and F_m indicates the comparator, $Z_o(s)$ denotes the open-loop output impedance of power stage, $G_{vg}(s)$, $G_{vd}(s)$, $G_{ii}(s)$, $G_{ig}(s)$ and $G_{id}(s)$ are the transfer functions of input voltage-to-output voltage, duty cycle-to-output voltage, output current-to-inductor current, input voltage-to-inductor current and duty cycle-to-inductor current respectively.

When the input voltage and the load current are in steady state, namely $\hat{i}_o(s) = \hat{v}_g(s) = 0$, the transfer functions of current loop $T_i(s)$ and voltage loop $T_v(s)$ can be expressed as:

$$T_i(s) = -G_{id}(s)R_i(1 + G_{com})F_m \quad (4)$$

$$T_v(s) = -G_{vd}(s)G_{com}F_mH \quad (5)$$

To analyze the characteristic of a multi-loop system, two transfer functions $T_1(s)$ and $T_2(s)$ are introduced to analyze the stability and calculate the output impedance respectively. According to Mason's gain formula, they are given by:

$$T_1(s) = T_i(s) + T_v(s) \quad (6)$$

$$T_2(s) = \frac{T_v(s)}{1 - T_i(s)} \quad (7)$$

3.2. Realization of Constant Output Impedance

Figure 4 shows the plots of open-loop output impedance Z_o and closed-loop output impedance Z_{oc} . It can be seen that Z_{oc} is smaller than Z_o at low frequencies because of the feedback function, but both of them are equal to ESR of output capacitor R_c at high frequencies. Therefore, by appropriate compensation, Z_{oc} at low frequencies can be adjusted to R_c and a constant output impedance can be achieved as AVP control shows. The detailed design is presented in the next paragraph.

Defining Z_{oi} as the output impedance with closed current loop and opened voltage loop, it is indicated in Figure 3(a). Based on Figure 3(b), it is written as follows:

$$Z_{oi} = \frac{Z_o(1 - T_i(s)) + G_{ii}(s)R_i(1 + G_{com})F_mG_{vd}(s)}{1 - T_i(s)} \quad (8)$$

While Z_{oc} is given by:

$$Z_{oc} = \frac{Z_o(1 - T_i(s)) + G_{ii}(s)R_i(1 + G_{com})F_mG_{vd}(s)}{1 - T_i(s) - T_v(s)} = \frac{Z_{oi}}{1 - T_2} \quad (9)$$

$$\text{When } T_2 \gg 1, \quad Z_{oc} = \frac{Z_{oi}}{1 - T_2} \approx -\frac{Z_{oi}}{T_2} \quad (10)$$

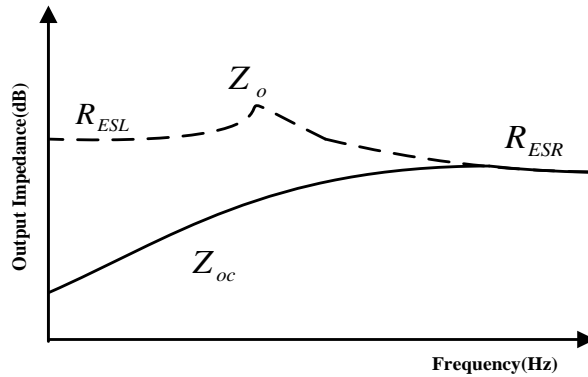


Figure 4. The Plots of Open-loop Output Impedance and Closed-loop Output Impedance

According to the derivation of Z_o , Z_{oi} and equation (10), the Bode plots of Z_o , Z_{oi} and ideal Z_{oc} , T_2 are shown in Fig. 5. To get a constant closed-loop output impedance Z_{oc} over the whole frequency domain, T_2 should satisfy the following requirements: an unity gain at ω_c , a slope of -20dB/decade below the frequency of ω_c , and a dominant pole at $(1+D)\omega_r$, where $\omega_r = 1/RC$, $\omega_L = R_L/L$, $\omega_o = D'/\sqrt{LC}$, $\omega_c = 1/RcC$, D is the duty ratio and $D' = 1 - D$.

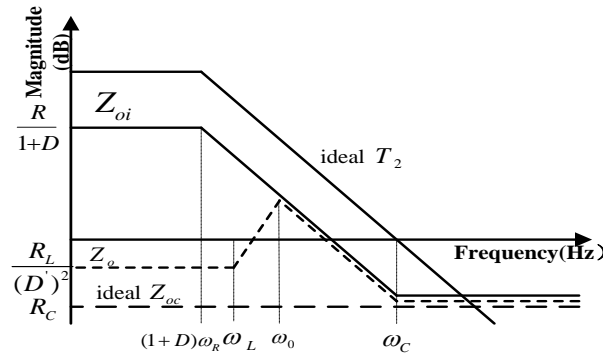


Figure 5. Bode Plots of Z_o , Z_{oi} and Ideal Z_{oc} , T_2

In equation (7), when $|T_i(s)| \gg 1$ and $|G_{com}| \gg 1$, $T_2(s)$ can be approximated as:

$$T_2(s) \approx -\frac{G_{vd}(s)H}{G_{id}(s)R_i} = -\frac{HD'R}{(1+D)R_i} \frac{(1+s/\omega_c)(1-s/\omega_z)}{1+s/(1+D)\omega_r} \quad (11)$$

where $\omega_z = (D')^2 R/DL$. It shows T_2 has a dominant pole at $(1+D)\omega_r$ and an unit-gain bandwidth at ω_c which are required for constant output impedance. As the constant output impedance $Z_{oc} = R_c$, and $|T_2| = HD'R/(1+D)R_i$ at low frequencies, the following equation is derived based on equation (10) and Figure 5:

$$|T_2| = \frac{HD'R}{(1+D)R_i} = \frac{|Z_{oi}|}{|Z_{oc}|} = \frac{R}{(1+D)R_c} \quad (12)$$

which means

$$R_i = D'HR_c \quad (13)$$

The value of resistance R_i could be chosen to realize constant output impedance according to the above equation, and smaller R_i leads smaller output impedance.

3.3. Effect of RHP Zero

It is easy to stabilize T_1 loop by compensation, however, T_2 contains a RHP zero ω_z which deteriorates system stability and the zero changes with load as shown in equation (11). In this section the effect of the RHP zero and the design of compensator are discussed.

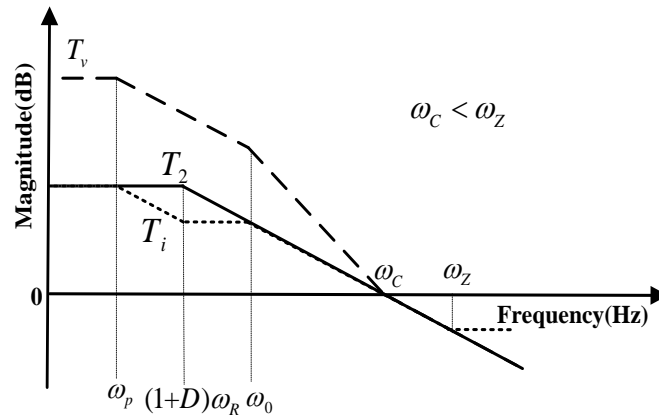


Figure 6. Amplitude Curves of T_i , T_v and T_2 when $\omega_c < \omega_z$

3.3.1. $\omega_c < \omega_z$: The compensated amplitude curves of T_i , T_v and T_2 are shown in Figure 6 when $\omega_c < \omega_z$. By setting the unit-gain bandwidth of T_i as ω_c , a desired and stable T_2 can be got. Besides, the second pole of the compensator should be designed at ω_z to keep T_2 a slope of -20dB/Dec. When the frequency is higher than ω_c , the magnitude plot of T_v aligns with that of T_2 .

3.3.2. $\omega_c > \omega_z$: As ω_z moves toward the origin when the load changes from light to heavy, the phase margins of T_1 and T_2 loops decrease. The value of droop resistance R_i is adjusted to increase the system stability. When $\omega_c > \omega_z$, the compensated amplitude curves of T_i , T_v and T_2 are illustrated in Figure 7(a). R_i is adjusting to set the bandwidth of T_2 at ω_z and the second pole of the compensator located at the frequency of ω_c . Thus, T_v can keep a -20dB/Dec slope. At frequencies between ω_z and ω_c , the magnitude curve of T_2 becomes flat and at the frequencies higher than ω_c , T_2 aligns with T_v with a slope of -20dB/Dec. The plots of Z_o , Z_{oi} and Z_{oc} are shown in Figure 7(b). It can be seen that Z_{oc} has a slight variation near the frequency of ω_c because of the lower gain and smaller bandwidth of T_2 .

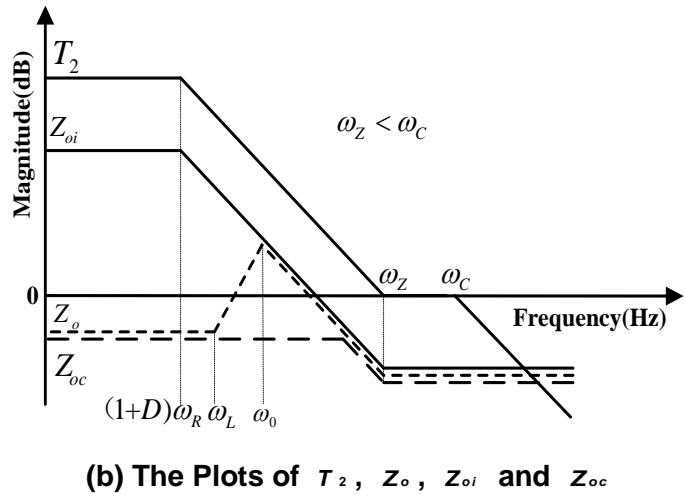
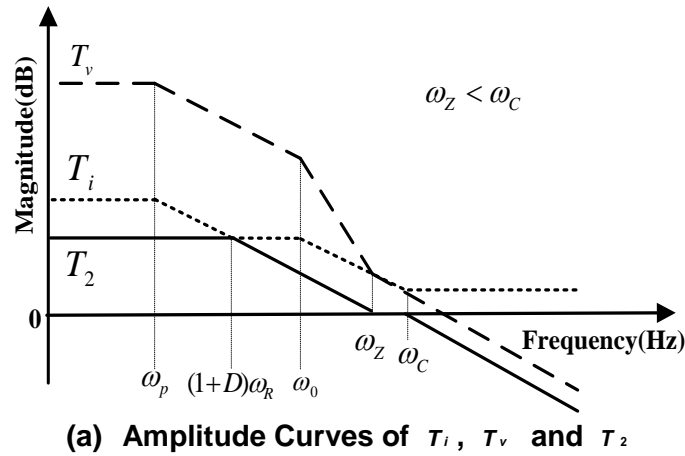
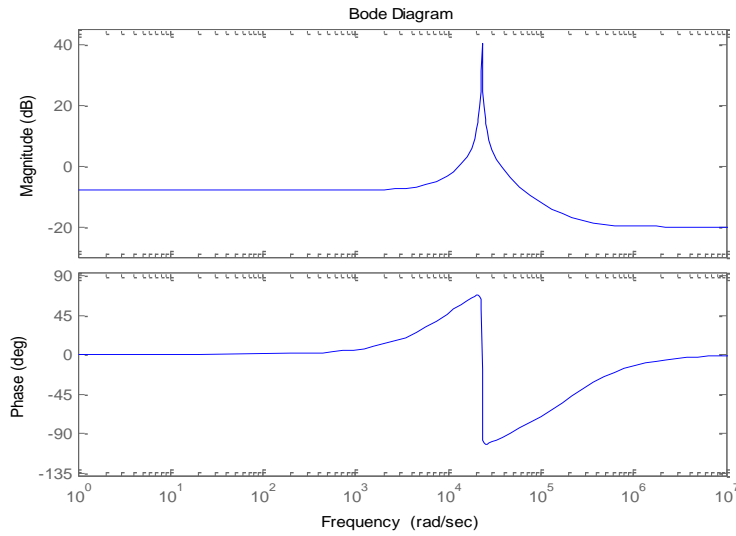


Figure 7. The Design of Compensator when $\omega_c > \omega_z$

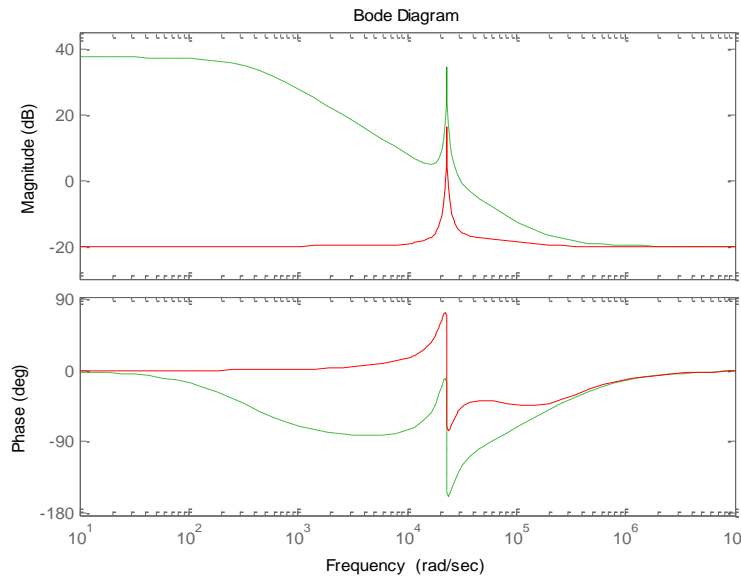
4. Simulation Results and Analysis

The parameters of the simulated buck-boost converter are listed below: input voltage $v_g = 6V$, duty ratio $D = 0.5$, output voltage $v_o = 6V$, filter inductance $L = 10\mu H$, filter capacitance $C = 47\mu F$, ESR of filter inductor $R_L = 0.1\Omega$, ESR of filter capacitor $R_C = 0.1\Omega$, load resistance $R = 100\Omega$ and switching frequency $f_s = 1MHz$.

Figure 8 compares the Bode plots of the open-loop output impedance and the closed-loop output impedance with AVP control. It shows that by applying AVP control technique, the system get a constant output impedance which equals to R_C .



(a) Open-loop Output Impedance



(b) The output impedance with AVP control (solid lines indicate Z_{oc} and dashed lines indicate Z_{oi})

Figure 8. The Bode Plots of Output Impedance

The Bode plots of output impedance with different cross frequencies f_{cross} are shown in Figure 9. When f_{cross} is close to resonant frequency f_o , an abnormal spike appears as the dashed line shows. It is efficient to reduce the resonant spike by increasing the cross frequency as the solid line shows. However, resonant spike still appears when the cross frequency is higher than f_c as the dotted line shows, therefore the optimal cross frequency is f_c .

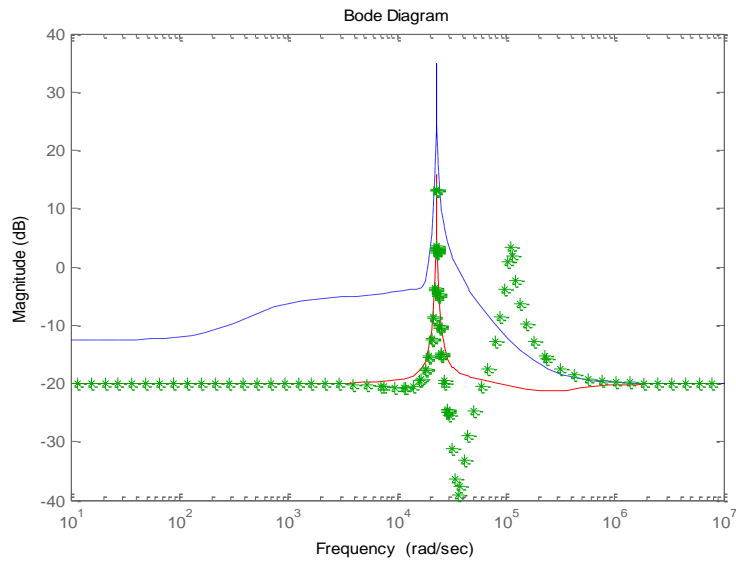
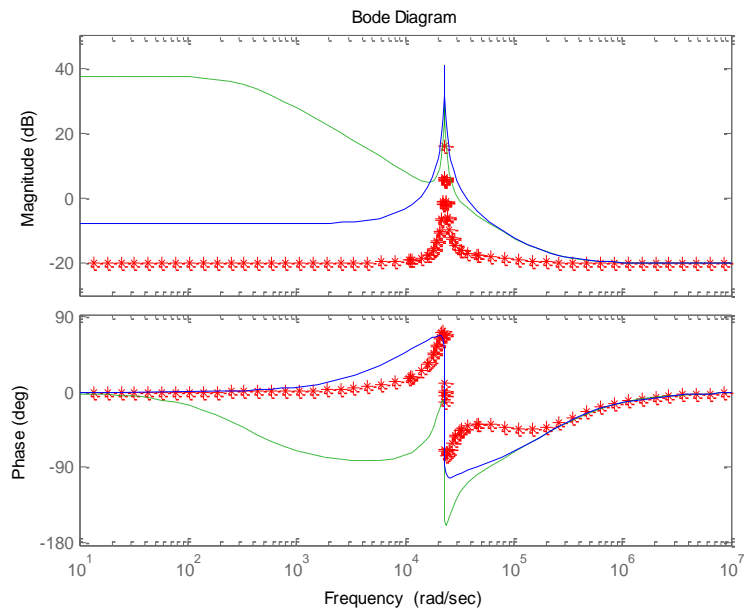
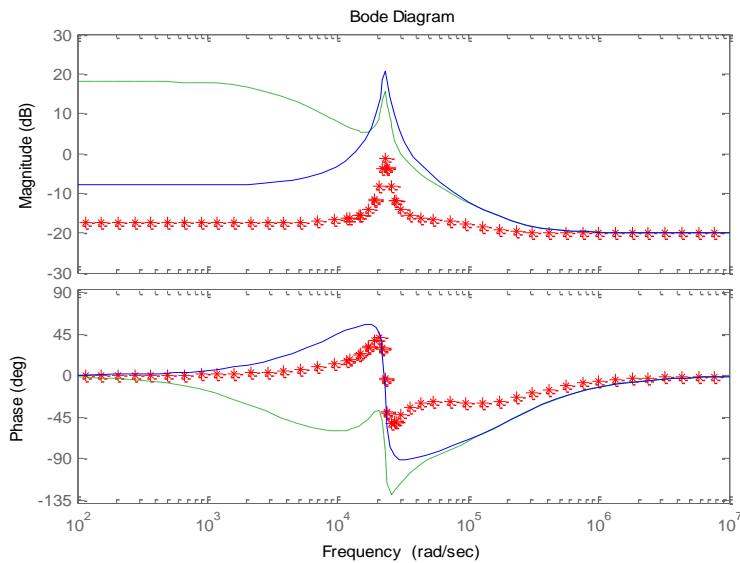


Figure 9. Bode Plots of Output Impedance with Different Cross Frequencies (dashed line: $f_{cross} = f_o$, solid line: $f_{cross} = f_c$ and dotted line: $f_{cross} = 10 f_c$)

Figure 10 shows the simulated output impedance of buck-boost converter at different loads. At light load when $i_o = 0.06 A$, the output impedance Z_{oc} equals to R_C . When the load changes from light to heavy such as $0.6A$, Z_{oc} at low frequencies is slightly larger than that at high frequencies because of a lower ω_z , as the dotted line in Figure 10(b) shows.



(a) The Bode plots at light load



(b) The Bode plots at heavy load

Figure 10. The Bode Plots at Different Loads (dotted lines indicate z_{oc} , dashed lines indicate z_{oi} , and Solid Lines Indicate z_o)

5. Conclusion

In this paper the design and system stability of buck-boost converter with AVP control is studied based on modeling. A method to achieve constant output impedance is proposed and through analyzing the RHP zero in buck-boost converter, this paper gives the design of compensation to keep stable with different RHP zeroes. The simulation results verify the analysis above. To imply AVP technique to converters with multiple RHP zeros will be studied and tested in the further work.

Acknowledgements

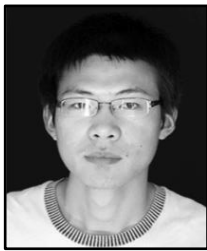
This paper is supported by State Key Laboratory of ASIC & System, Fudan University (12KF001), Fudan University State Key Laboratory of ASIC & System Senior Visiting Scholarship (11FG029) and Science and Research Funds of Hefei University of Technology (2013HGXI0192).

References

- [1] A.Kumar, S. Li, and N.K. Jha, "System-Level Dynamic Thermal Management for High-Performance Microprocessors", IEEE Trans. Computer-Aided Design of Integrated Circuits and Systems, vol.27, no.1, (2008), pp. 96-108.
- [2] S. Narasimhan, K. Kunaparaju, and S. Bhunia, "Healing of DSP Circuits Under Power Bound Using Post-Silicon Operand Bitwidth Truncation", IEEE Trans. Circuits and Systems I: Regular Papers, vol.59, no.9, (2012), pp. 1932-1941.
- [3] K. Y. Cheng, F. Yu, P. Mattavelli and F.C. Lee, "Characterization and Performance Comparison of Digital V2-Type Constant On-Time Control for Buck Converters", 2010 IEEE 12th Workshop on Control and Modeling for Power Electronics (COMPEL), (2010) June, 28-30.
- [4] M. Castilla, L. Garcia De Vicuna, J.M. Guerrero, J. Matas and J. Miret, "Designing VRM Hysteretic Controllers for Optimal Transient Response", IEEE Trans. Power Electronics, vol.54, no.3, (2007), pp.1726-1738.

- [5] K. I. Hwu, and T. J. Peng, "A Novel Buck-Boost Converter Combining KY and Buck Converters", IEEE Trans. Power Electronics, vol.27, no.5, (2012), pp. 2236-2241.
- [6] M. Lee, D. Chen, K. Huang, C. W. Liu, and B. Tai, "Modeling and Design for a Novel Adaptive Voltage Positioning(AVP) Scheme for Multiphase VRMs", IEEE Trans. Power Electronics, vol.23, no.4, (2008), pp. 1733-1742.
- [7] C. J. Chen, C. S. Huang, D. Chen, M. Lee, and E.K. -L. Tseng, "Modeling and Design Considerations of a Novel High-Gain Peak Current Control Scheme to Achieve Adaptive Voltage Positioning(AVP) for DC Power Converters", IEEE Trans. Power Electronics, vol.24, no.12, (2009), pp. 2942-2950.
- [8] Q. Ying, X. Y. Chen and L. Helen, "Digital Average Current-Mode Control using Current Estimation and Capacitor Charge Balance Principle for DC-DC Converters Operating in DCM", IEEE Trans. Power Electronics, vol.25, no.6, (2010) ,pp. 1537-1545.
- [9] A. A. Boora, F. Zare, and A. Ghosh, "Multi-Output Buck-Boost Converter with Enhanced Dynamic Response to Load and Input Voltage Changes", IET Power Electronics, vol.4, no.2, (2011), pp. 194-208.
- [10] H. H. Huang, C. Y. Hsieh, J.Y. Liao and K. H. Chen, "Adaptive Droop Resistance Technique for Adaptive Voltage Positioning in Boost DC-DC converters", IEEE Trans. Power Electronics, vol.26, no.7, (2011), pp. 1920-1932.
- [11] M. Lee, D. Chen, K. Huang, C. W. Liu, and B. Tai, "Modeling and Design for a Novel Adaptive Voltage Positioning Scheme for Multiphase VRMs", IEEE Trans. Power Electronics, vol.23, no.4, (2008), pp. 1733-1742.
- [12] Y. J. Chen, D. Chen, Y. C. Lin, C. J. Chen, and C. H. Wang, "A Novel Constant On-Time Current-Mode Control Scheme to Achieve Adaptive Voltage Positioning for DC-DC Power Converters", IECON 2012-38th Annual Conference on IEEE Industrial Electronics Society, (2012), October,25-28.

Authors



Fei Deng, received the B. S. degree in material physics from Anhui University, Hefei, China, in 2011. Now he is studying for the M. S. degree in microelectronics in Hefei University of Technology, Heifei, China. His research interests include DC-DC converter.



Guangjun Xie, received the B. S., M. S. degrees in microelectronics from Hefei University of Technology, Hefei, China, in 1992, 1995 respectively, and the PH.D. degree in signal and information processing from University of Science and Technology of China, Hefei, China, in 2002. He is currently a Professor in School of Electronic Science and Applied Physics, Hefei University of Technology. His research interests include integrated circuit design and quantum circuit.



Xin Cheng, received the B. S., M. S. degrees in microelectronics from Hefei University of Technology, Hefei, China, in 2006, 2009 respectively, and the PH.D. degree in microelectronics from Institute of Electronics, Chinese Academy of Sciences, Beijing, China, in 2012. Now she serves as a lecturer in School of Electronic Science and Applied Physics, Hefei University of Technology. Her research interests include DC-DC converter and analog integrated circuit design.

